The American Journal of Pathology, Vol. 191, No. 6, June 2021

The American Journal of
PATHOLOGY
ajp.amjpathol.org

VASCULAR BIOLOGY, ATHEROSCLEROSIS, AND ENDOTHELIUM BIOLOGY

Spatial Distribution of Mast Cells Regulates Asymmetrical Angiogenesis at the Ocular Surface

WonKyung Cho, Sharad K. Mittal, Elsayed Elbasiony, and Sunil K. Chauhan

From the Schepens Eye Research Institute of Mass Eye and Ear, Harvard Medical School, Boston, Massachusetts

Accepted for publication February 17, 2021.

Address correspondence to Sunil K. Chauhan, D.V.M., Ph.D., Schepens Eye Research Institute of Mass Eye and Ear, Harvard Medical School, 20 Staniford St., Boston, MA 02114. E-mail: sunil_chauhan@meei.harvard.edu.

Mast cells, historically known for their function as effector cells in the induction of allergic diseases, reside in all vascularized tissues of the body, particularly, in proximity to blood and lymphatic vessels. Despite being neighboring sentinel cells to blood vessels, whether the spatial distribution of mast cells regulates the degree of angiogenesis remains to be investigated. Herein, an asymmetrical distribution of mast cells was shown at the murine ocular surface, with the higher number of mast cells distributed along the nasal limbus of the cornea compared with the temporal side. Using a well-characterized murine model of suture-induced corneal neovascularization, insult to the nasal side was shown to result in more extensive angiogenesis compared with that to the temporal side. To directly assess the impact of the spatial distribution of mast cell on angiogenesis, neovascularization was induced in mast cell–deficient mice (cKit$^{w\text{-}sh}$). Unlike the wild-type (C57BL/6) mice, cKit$^{w\text{-}sh}$ mice did not show disproportionate growth of corneal blood vessels following the temporal and nasal insult. Moreover, cromolyn-mediated pharmacologic blockade of mast cells at the ocular surface attenuated the asymmetrical nasal and temporal neovascularization, suggesting that spatial distribution of mast cells significantly contributes to angiogenic response at the ocular surface. *(Am J Pathol 2021, 191: 1108–1117; https://doi.org/10.1016/j.ajpath.2021.02.016)*

A transparent cornea, devoid of any blood vessels, is essential to maintaining visual acuity.[1,2] Corneal neovascularization, characterized by abnormal new blood vessel growth from preexisting limbal vessel structures, occurs in various corneal pathologies, including inflammatory disorders, trauma, and corneal graft rejection.[3,4] Pathologic insults lead to a disruption of the equilibrium of pro-angiogenic and anti-angiogenic factors, resulting in proliferation and migration of vascular endothelial cells to form new blood vessels.[5] Interestingly, the pathologic growth of blood vessels is not always evenly distributed throughout the cornea. Ocular surface conditions, including peripheral hypertrophic subepithelial corneal opacification and pterygium, characterized by pathologic angiogenesis, have long been clinically observed to predominantly affect the nasal side of the cornea.[6–8] Despite such observations, the underlying mechanism that may contribute to the uneven distribution of neovascularization in tissues, such as the cornea, is yet to be uncovered.

Mast cells, the tissue-resident cells, are present throughout vascularized tissues in the body, especially in abundance around the blood and lymph vessels.[9,10] At the ocular surface, mast cells are distributed in the peripheral cornea, limbus, and conjunctiva.[11,12] On activation, mast cells degranulate and release preformed and newly synthesized inflammatory mediators into the microenvironment.[10] Granules are composed of various growth factors, cytokines, amines, and enzymes such as tryptase and β-hexosaminidase.[9,13] The role of mast cells in ocular allergy is well established, and the use of a mast cell inhibitor, cromolyn sodium, to manage allergic symptoms, is a common practice in the clinic. Apart from their well-established role in allergy, mast cells also regulate innate and adaptive immune responses and angiogenesis.[14,15]

Ocular surface mast cells promote corneal neovascularization, in part, by secreting high levels of vascular endothelial growth factor-A.[16] In the current study, a series of

Supported by the NIH grants R01EY029727 (S.K.C.) and P30EY003790.

Disclosures: None declared.

https://doi.org/10.1016/j.ajpath.2021.02.016

experiments were conducted to investigate whether mast cells contribute to the observed asymmetry in vessel growth between the nasal and temporal side of the cornea. Specifically, the effect of the spatial distribution of mast cells were investigated on pathologic vessel formation using a well-characterized murine model of inflammatory corneal neovascularization and genetically modified mast cell–deficient cKit$^{w\text{-}sh}$ mice. Herein, suture placement on the nasal side resulted in more extensive corneal neovascularization compared with that on the temporal side. Moreover, a higher number of mast cells were observed on the nasal half of the cornea compared with the temporal half. However, mast cell deficiency and pharmacologic blockade of mast cell activation abrogated the difference in the degree of angiogenesis following nasal and temporal insult, suggesting a critical contribution of mast cells in promoting disproportionate angiogenic response at the ocular surface.

Materials and Methods

Animals

BALB/c mice, aged 6 to 8 weeks, were used for the described experiments. A fully congenic cKit$^{w\text{-}sh}$ mouse strain on a C57BL/6J genetic background (stock number 012861) and sex- and age-matched C57BL/6J mice were purchased from Jackson Laboratory (Bar Harbor, ME).[17] Littermates were used for each set of experiments. cKit$^{w\text{-}sh}$ mice were confirmed for their deficiency in mast cells at the ocular surface and in the peritoneum and for their comparable generation of total CD45^{+} cells and myeloid cells in the bone marrow compared with wild-type mice.[17,18] There is an increased accumulation of neutrophils and platelets in different lymph organs of cKit$^{w\text{-}sh}$.[19] All protocols were approved by the Animal Care and Use Committee of Schepens Eye Research Institute. The mice were housed in the Schepens Eye Research Institute animal vivarium and treated according to the Association for Research in Vision and Ophthalmology Guidelines for Use of Animals in Ophthalmic and Vision Research.

Corneal Neovascularization Model

Corneal neovascularization was induced by placing a single intrastromal suture on anesthetized mice, as previously described.[20,21] Briefly, a single figure-of-eight suture was intrastromally placed on either the nasal or the temporal side of the cornea, 1.0 mm from the limbal area using 11.0 nylon sutures (MANI, Tochigi, Japan). The sutures remained in the cornea and induced inflammation and neovascularization (Figure 1). Following suture placement, a triple antibiotic ointment was applied topically. To subside suture-induced pain, buprenorphine was administered via s.c. injection. Ocular surface tear wash (5 μL/wash) was collected at 0, 1, 3, and 6 hours after suture placement to measure mast cell activation. Mice were clinically assessed using a slit lamp, and subsequently, on day 4, were euthanized, and their corneas (including the corneal limbus and conjunctiva) were harvested for further analysis.

Mast Cell Inhibitor Administration

Three microliters of phosphate-buffered saline (PBS) or 2% sodium cromolyn in PBS (Sigma-Aldrich Corp., St. Louis, MO) was administered topically to sutured corneas at five time points on the day of suture placement (−3, −1, 1, 3, and 6 hours postoperatively). Thereafter, PBS or cromolyn was administered topically five times per day (every 3 hours) for 4 days.

Tissue Lysate Preparation

Corneas were harvested and lysed using the freeze-thaw method. Briefly, corneas were digested by placing the corneas alternatively in dry ice and 37°C water bath. Corneal tissue was mechanically lysed using a pellet pestle (Life Sciences, Waltham, MA) between every cycle. A total of seven complete freeze-thaw cycles were completed before centrifuging the cells. The supernatant was collected for tryptase and β-hexosaminidase analysis.

Tryptase Assays

Mast Cell Degranulation Assay Kits (Sigma-Aldrich) were used to quantify levels of tryptase enzyme. The kit detects the chromophore p-nitroaniline cleaved from the labeled substrate tosyl-gly-pro-lys-p-nitroaniline.[22] In brief, ocular surface tear wash or corneal lysates were incubated with 0.1 mg/mL tosyl-gly-pro-lys-p-nitroaniline (substrate) for 3 hours at 37°C. A SpectraMax Plus 384 Microplate Reader (Molecular Devices, San Jose, CA) was used to quantify free p-nitroaniline at 405 nm.

β-Hexosaminidase Assays

Levels of β-hexosaminidase enzyme were quantified using β-n-acetylglucosaminidase assay kits (Sigma-Aldrich). The kit measures the level of 4-nitrophenyl N-acetyl-β-D-glucosaminide hydrolysis.[23] In brief, corneal lysates or ocular surface tear wash was incubated with 0.1 mg/mL 4-nitrophenyl N-acetyl-β-D-glucosaminide (substrate) for 1 hour at 37°C. The enzyme-substrate reaction was stopped with 5 mg/mL sodium carbonate, and absorbance at 405 nm was measured using SpectraMax Plus 384 Microplate Reader (Molecular Devices). β-Hexosaminidase levels were estimated using the formula: U/mL = (A405sample − A405blank) × 0.05 × 0.3 × Dilution Factor/A405 standard × time × volume of sample in milliliters.

Immunohistochemistry

Corneas with limbus were harvested and immunostained, as previously described.[24,25] Briefly, corneal stroma and epithelium were separated after EDTA treatment for 30 minutes at 37°C, and the stroma was fixed using 4% paraformaldehyde. Tissues were incubated at 4°C with fluorescein isothiocyanate–conjugated CD31 (Biolegend, San Diego, CA) overnight. To stain for avidin, the harvested cornea was fixed using 4% paraformaldehyde and was subsequently incubated at 4°C with Texas red–conjugated avidin (ThermoFisher, Waltham, MA) for 6 hours. Stained corneas were whole mounted on slides using VECTASHIELD mounting medium with DAPI (Vector Laboratories, Burlingame, CA) and visualized using a confocal microscope (Leica TCS-SP5; Buffalo Grove, IL). The area covered by blood vessel ($CD31^+$) and the number of mast cells ($avidin^+$) was calculated using ImageJ version 1.52v software (NIH, Bethesda, MD; *https://imagej.nih.gov/ij*, last accessed November 20, 2020).[26]

Slit-Lamp Microscopy

Slit-lamp biomicroscopy was used to clinically evaluate corneal neovascularization following suture placement and to acquire images.[27] The slit-lamp analysis was performed on days 2 and 4 after suture placement. Slit-lamp images were converted into binary images, and vascular density as percentage area of the vessels in the total cornea was calculated using the vessel analysis plugin in ImageJ version 1.52v.

Statistical Analysis

Unpaired two-tailed *t*-tests were used to compare means between two groups. The significance level was set at $P < 0.05$. Data are presented as the means ± SEM. The results shown are representative of at least three independent experiments. Sample sizes were estimated on the basis of previous studies on corneal angiogenesis.[16,27]

Results

Increased Neovascularization following Suture Placement on the Nasal Side of the Cornea

To investigate the degree of neovascularization depending on the site of insult, a model of inflammatory corneal neovascularization was used.[28] A single intrastromal figure-of-eight suture 1 mm from the limbus was placed on either the nasal or the temporal side of the cornea of BALB/c mice (Figure 1A). Nonsutured corneas served as controls. Corneal neovascularization was clinically assessed every 2 days using a slit-lamp biomicroscope (Figure 1B). Binary images from slit-lamp images were generated to quantify vascular density using the ImageJ version 1.52v software. Nasal suture resulted in significantly more neovascularization compared with temporal suture on day 4 after suture placement ($P = 0.01$) (Figure 1C). To quantify the growth of the microvessels not visible to the naked eye, corneas were harvested on day 4 for immunohistochemistry analysis. Whole-mounted corneas were immunostained with fluorochrome-conjugated CD31, and blood vessel growth was measured by calculating the vessel area covered by the new branching blood vessels using ImageJ version 1.52v software. Consistent with previous clinical observations,[6,7] significantly higher nasal neovascularization was observed compared with temporal neovascularization following suture placement ($P = 0.04$) (Figure 1D). These results suggest that the location of the insult mediates the degree of neovascularization, specifically that suture placed on the nasal side results in increased neovascularization compared with that placed on the temporal side of the cornea.

Spatial Distribution of Mast Cells at the Ocular Surface

Having observed greater corneal neovascularization following nasal suture, the mechanism underlying the difference in blood vessel growth was investigated. Mast cells, distributed along the limbal area of the cornea,[18] are associated with angiogenesis in various pathologies[15,29]; therefore, the hypothesis that mast cell distribution and activation account for the difference in neovascularization was tested. To investigate mast cell distribution, naïve corneas were harvested with limbus and cut into nasal and temporal halves. Each half of the cornea was immunostained with fluorochrome-conjugated avidin, which specifically binds to mast cells (Figure 2A). The numbers of $avidin^+$ mast cells were quantified using ImageJ version 1.52v software. A significantly higher number of mast cells were distributed along the limbus of the nasal half of the cornea compared with the temporal half ($P = 0.02$) (Figure 2B). To further confirm the spatial distribution of mast cells, nasal and temporal halves of the naïve cornea were lysed, and levels of mast cell–specific markers, tryptase, and β-hexosaminidase, were quantified.[30] The nasal half showed significantly higher levels of tryptase and β-hexosaminidase, compared with the temporal half ($P = 0.02$ and $P = 0.007$, respectively) (Figure 2C). To assess whether this dichotomy of mast cell distribution perpetuates during neovascularization, tear wash was collected following suture placement to analyze secretion of tryptase and β-hexosaminidase (Figure 2D). The suture placed on the nasal side resulted in a higher fold increase in tryptase [4.3-fold versus 1.4-fold (temporal); $P = 0.0002$] and β-hexosaminidase levels [2.1-fold versus 1.1-fold (temporal); $P = 0.006$], compared with that placed on the temporal side. Our data indicate a higher distribution of mast cell on the nasal half of the cornea, suggesting that observed differences in suture-induced mast cell activation result from the underlying difference in spatial distribution of mast cells.

Mast Cell Deficiency Abrogates Asymmetrical Nasal and Temporal Neovascularization

Having observed increased neovascularization and enhanced mast cell activation following insult to the nasal side, whether

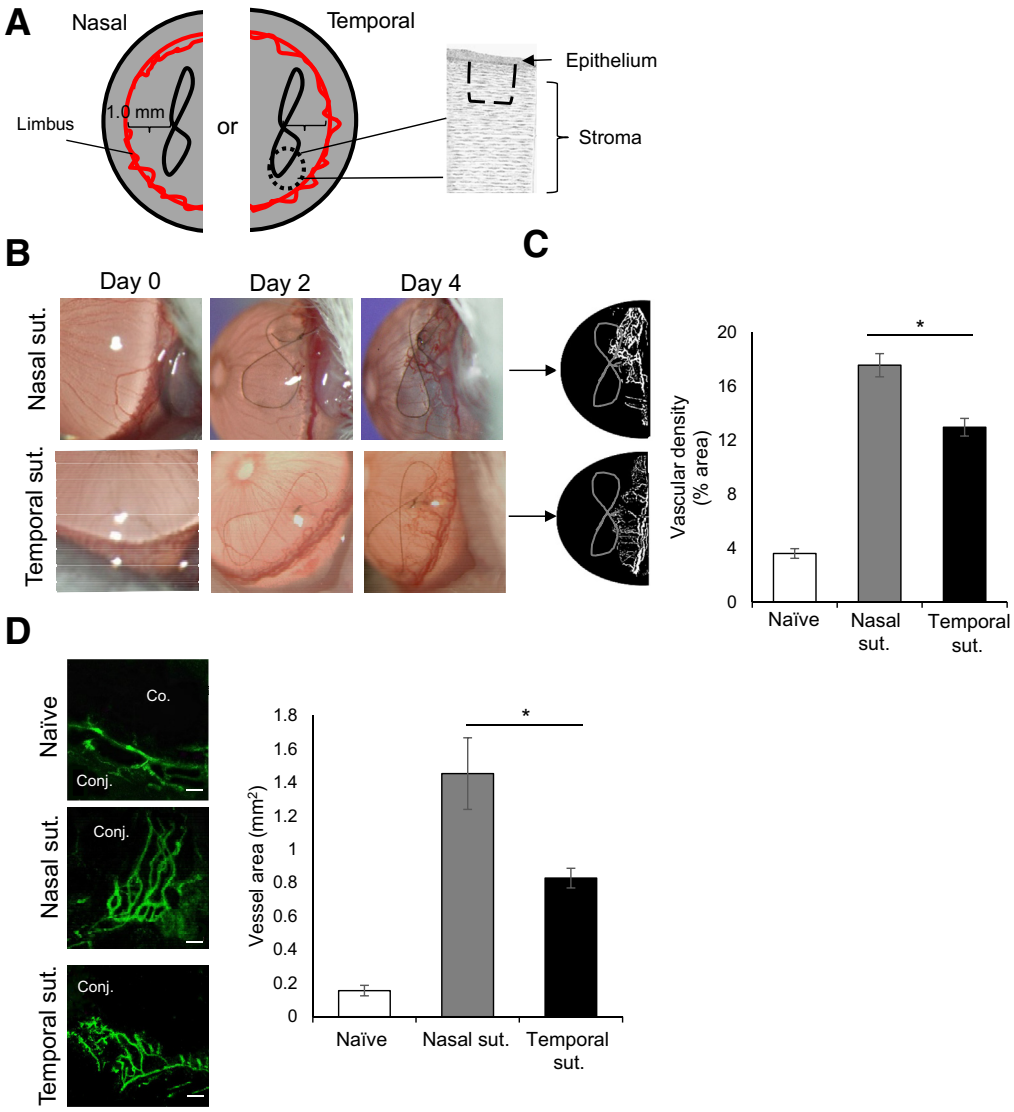

Figure 1 Suture (sut.) placement on the nasal side results in increased neovascularization. **A:** Schematic drawing of the single intrastromal suture placement (**dashed lines**) 1.0 mm from the limbal area on either the temporal or the nasal side of the cornea. **B:** Representative slit-lamp biomicroscope images of corneas with sutures on the nasal or temporal side on day 0 (naïve cornea), 2, and 4 after suture placement in BALB/c mice. **C:** Binary images (**left side**) and cumulative bar chart (**right side**) depicting the vascular density of corneal neovascularization. Slit-lamp images were converted into binary images, and vascular density as percentage area of the vessels in the total cornea was calculated using the vessel analysis plugin in ImageJ version 1.52v software. **D:** Representative immunohistochemistry micrographs (**left side**) and cumulative bar chart (**right side**) showing vessel area in naïve, nasal, and temporal sutured corneas. Corneas were harvested on day 4 after suture placement and immunostained with CD31 (fluorescein isothiocyanate). ImageJ version 1.52v software was used to quantify the vessel area. Representative data from three independent experiments are shown, and each experiment consisted of four animals. Data are represented as means ± SEM (**C** and **D**). *$P < 0.05$ (*t*-test). Scale bar = 100 μm (**D**). Co., cornea; Conj., conjunctiva.

the spatial distribution of mast cells was critical to the asymmetrical angiogenic response was assessed. To determine this, corneal neovascularization was indiced in mast cell–deficient mice (cKit$^{w\text{-}sh}$) and wild-type C57BL/6 mice (control). cKit$^{w\text{-}sh}$ mice are deficient in mast cells at the ocular surface and in the peritoneum with comparable generation of total CD45^{+} cells and myeloid cells in the bone marrow compared with wild-type mice.[17,18] However, there is an increased accumulation of neutrophils and platelets in different lymph organs of cKit$^{w\text{-}sh}$.[19] Immunohistochemistry analysis using avidin staining confirmed the deficiency of mast cells at the ocular surface in cKit$^{w\text{-}sh}$ mice (Figure 3A). Neovascularization was clinically assessed in naïve cornea following suture placement on days 2 and 4 using a slit-lamp biomicroscope (Figure 3B). Slit-lamp images were converted into binaries using ImageJ version 1.52v software to quantify vascular density. As in BALB/c mice (Figure 1B), C57BL/6 mice showed a higher degree of neovascularization following suture placement on the nasal side compared with that on the temporal side (Figure 3B). However, no significant difference

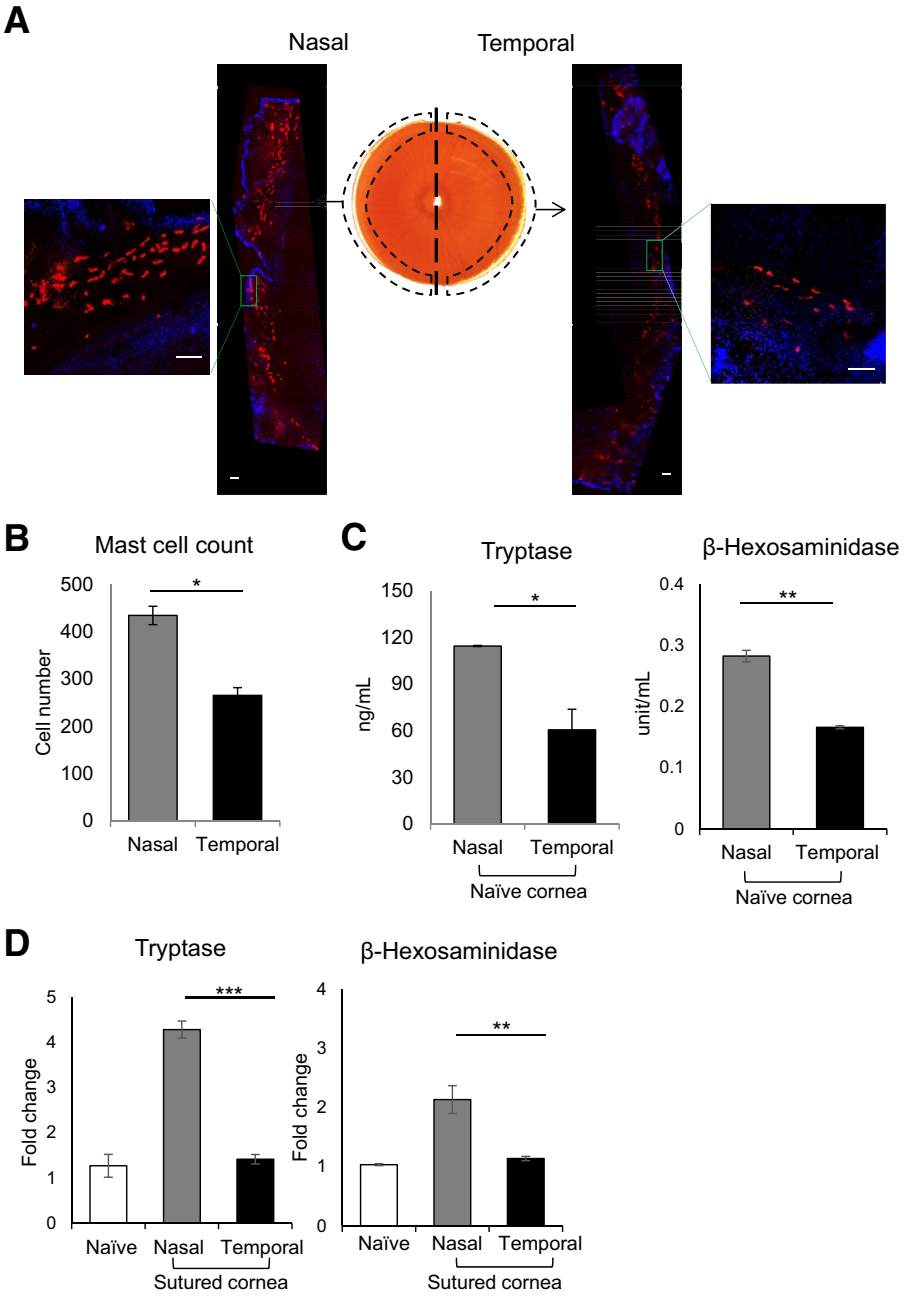

Figure 2 Enhanced distribution and activation of mast cells at the nasal side of the cornea. **A:** Representative immunohistochemistry micrograph of BALB/c murine cornea whole mounted and stained with fluorescent-conjugated avidin (Texas red) to visualize mast cells. **B:** Cumulative bar chart showing the number of mast cells (avidin^{+}) on the nasal and temporal side of the cornea. The cornea was cut into nasal and temporal halves at harvesting. ImageJ version 1.52v software was used to quantify the number of mast cells. **C:** Levels of tryptase (**left side**) and β-hexosaminidase (**right side**) of lysates of nasal and temporal halves of naïve corneas. **D:** Ocular surface tear wash was collected at 0, 1, 3, and 6 hours following nasal or temporal suture placement (5 μL/wash) to measure mast cell activation markers tryptase (**left side**) and β-hexosaminidase (**right side**). Tear wash was collected from naïve mice as control. Representative data from three independent experiments are shown, and each experiment consisted of four animals. Data are represented as means ± SEM (**B**–**D**). $*P < 0.05$, $**P < 0.01$, and $***P < 0.001$ (*t*-test). Scale bar = 100 μm (**A**).

in corneal neovascularization was observed following nasal and temporal suture in cKit$^{w\text{-}sh}$ mice on day 4 (Figure 3, B and C). Collectively, current data suggest that asymmetrical neovascularization is dependent on the spatial distribution of mast cells at the ocular surface.

Pharmacologic Blockade of Mast Cells Attenuates the Spatial Angiogenic Response at the Ocular Surface

Finally, to assess whether inhibiting mast cell activation nullifies the difference in the degree of neovascularization,

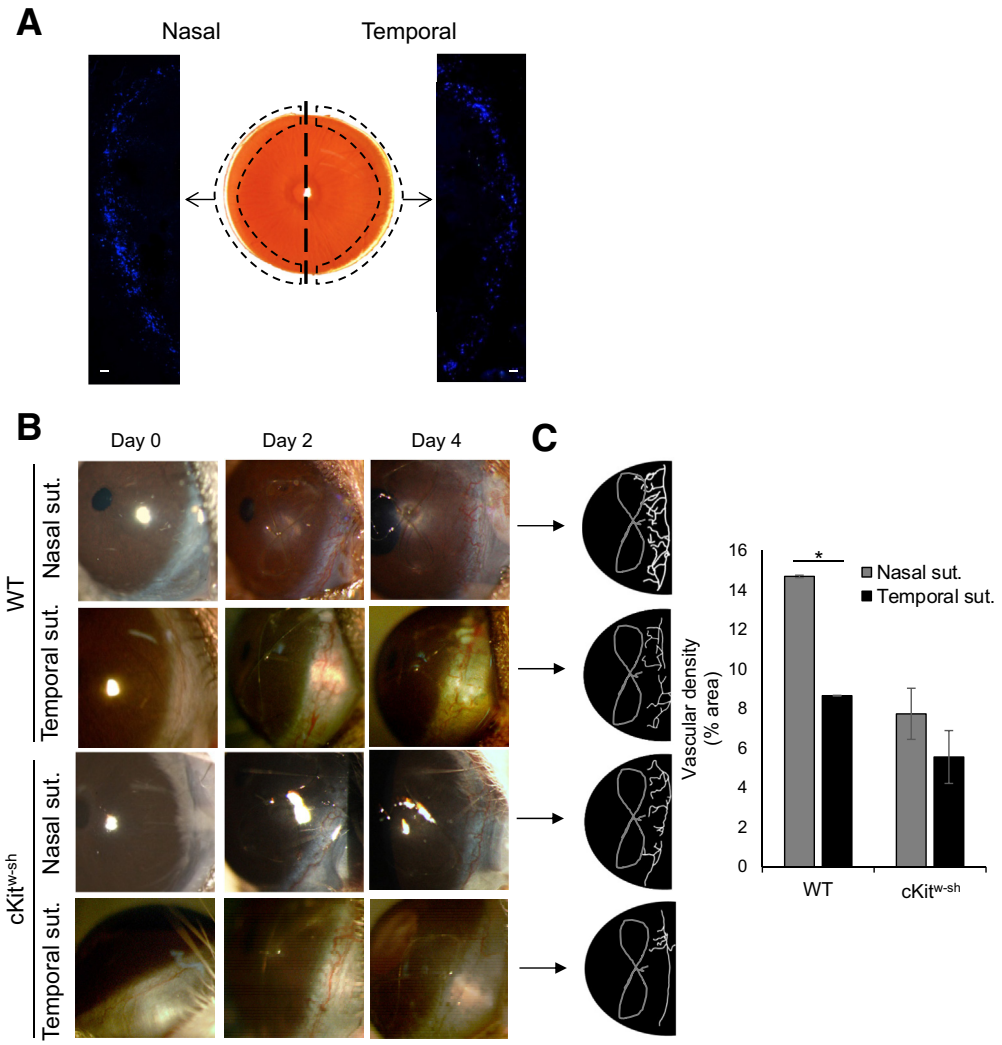

Figure 3 Comparable neovascularization at nasal and temporal cornea in mast cell–deficient mice. **A:** Representative immunohistochemistry micrograph of cKit$^{w\text{-}sh}$ mice cornea whole mounted and stained with fluorescent-conjugated avidin (Texas red) to visualize deficiency of mast cells. **B:** Representative slit-lamp biomicroscope images of nasal or temporal sutured corneas of wild-type (WT; C57BL/6) and cKit$^{w\text{-}sh}$ mice on day 0 (naïve cornea), 2, and 4 after suture. **C:** Binary images (**left side**) and cumulative bar chart (**right side**) depicting the vascular density of corneal neovascularization. Slit-lamp images were converted into binary images, and vascular density as percentage area of the vessels in the total cornea was calculated using the vessel analysis plugin in ImageJ version 1.52v software. Representative data from three independent experiments are shown, and each experiment consisted of three animals. Data are represented as means ± SEM (**C**). *$P < 0.05$ (*t*-test). Scale bar = 100 μm (**A**). Sut., suture.

corneas were topically treated with 2% cromolyn, a clinically used mast cell stabilizer.[31] Corneas were treated, as outlined in the experimental design, with cromolyn or PBS control (Figure 4A). Topical treatment of cromolyn significantly suppressed ocular surface mast cell activation, as confirmed by lower levels of tryptase in cromolyn-treated corneas (Figure 4B). Corneal neovascularization was clinically assessed every 2 days using a slit-lamp biomicroscope (Figure 4C). Slit-lamp images were converted into binary images to measure vascular density using ImageJ version 1.52sv software. Cromolyn treatment abrogated the difference in suture-induced nasal and temporal neovascularization, with a dramatic reduction in total vessel growth at the ocular surface (Figure 4D). Furthermore, cromolyn-mediated attenuation of asymmetrical neovascularization was confirmed using immunohistochemistry analysis of corneas harvested on day 4 after suture placement. Consistent with the slit-lamp observation, no significant difference was observed in the suture-induced growth of CD31$^+$ vessels between the nasal and temporal side following cromolyn treatment (Figure 4E). In addition, the effect of cromolyn on vascular endothelial cells was tested using an *in vitro* culture system. No difference in the proliferation of vascular endothelial cells between PBS- and cromolyn-treated cultures (Supplemental Figure S1) was observed. Taken together, the data demonstrate that pharmacologic blockade of mast cells abrogates the difference in the degree of suture-induced neovascularization.

Discussion

Corneal neovascularization, a prevalent adverse effect of various ocular surface conditions, disrupts the corneal

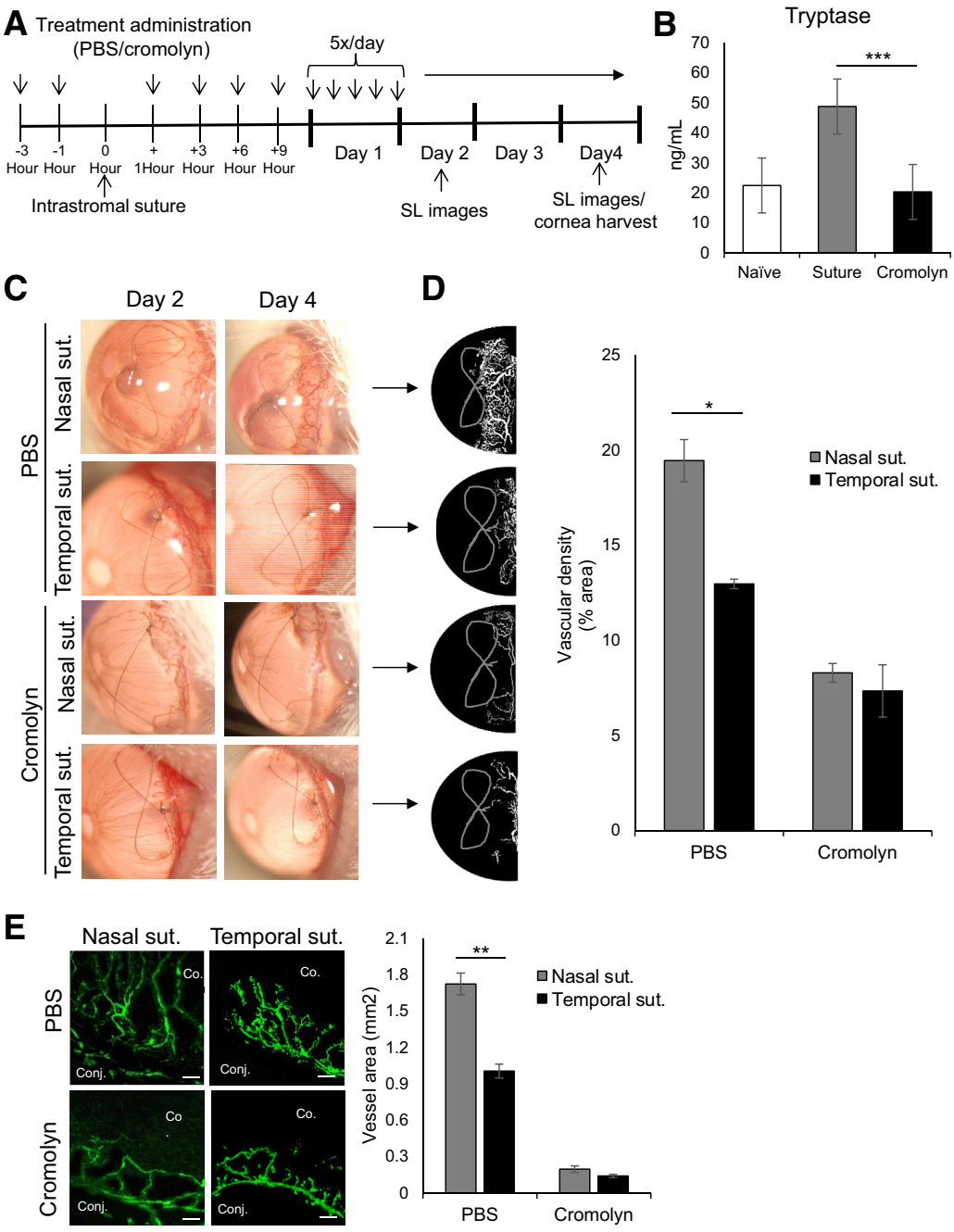

Figure 4 Cromolyn-mediated mast cell inhibition nullifies the asymmetrical distribution of nasal and temporal neovascularization. **A:** Schematic experimental design showing the time points of treatment administration in BALB/c mice with intrastromal sutures (suts.). Mice were treated with phosphate-buffered saline (PBS) or 2% cromolyn (3 μL/treatment). After 4 days, corneas were harvested for immunohistochemistry analysis of corneal neovascularization. **B:** Ocular surface tear wash (5 μL/wash) was collected at 0, 1, 3, and 6 hours following PBS or cromolyn treatment of corneas with sutures to measure tryptase, a mast cell activation marker. **C:** Representative slit-lamp biomicroscope images of corneas with sutures on nasal or temporal side following PBS or cromolyn treatment on days 2 and 4 after suture placement. **D:** Binary images (**left side**) and cumulative bar chart (**right side**) depicting the vascular density of corneal neovascularization. Slit-lamp images were converted into binary images, and vascular density as percentage area of the vessels in the total cornea was calculated using the vessel analysis plugin in ImageJ version 1.52v software. **E:** Representative immunohistochemistry micrographs (**left side**) and cumulative bar chart (**right side**) showing vessel area in nasal or temporal sutured corneas treated with PBS or cromolyn. Corneas were harvested on day 4 after suture placement and immunostained with CD31 (fluorescein isothiocyanate). ImageJ version 1.52v software was used to quantify the vessel area. Representative data from three independent experiments are shown, and each experiment consisted of four animals. Data are represented as means ± SEM (**B**, **D**, and **E**). $*P < 0.05$, $**P < 0.01$, and $**P < 0.001$ (*t*-test). Scale bar = 100 μm (**E**). Co., cornea; Conj., conjunctiva; SL, slit lamp.

clarity by inducing persistent inflammation.[32,33] This study advances our understanding of corneal neovascularization and the contribution of the spatial distribution of mast cells to the disproportionate angiogenic response. Specifically, the current data show that i) suture placement on the nasal side results in greater corneal neovascularization than that on the temporal side, ii) higher number of mast cells are distributed on the nasal side of the cornea, iii) mast cell

deficiency results in comparable levels of corneal neovascularization following nasal and temporal insult, and iv) pharmacologic blockade of mast cells abrogates the difference in degree of suture-induced nasal and temporal neovascularization.

Despite disproportionate neovascularization affecting various corneal pathologies, only a few studies have investigated the spatial distribution of pathologic neovascularization across the cornea. Pterygium, a thickened triangular tissue growth of the cornea, is marked by a high degree of vascularization, particularly on the nasal side.[7,34] Similarly, significantly more neovascularization was observed on the nasal side of the cornea following suture placement compared with the temporal side. This study shows, for the first time, that spatial distribution of mast cells contributes to the nasal preferences of corneal neovascularization.

Mast cells, the tissue-resident secretory cells, have been implicated in various pathologic conditions, including angiogenesis.[35,36] The current data, consistent with previous studies, show that mast cells are primarily located around the limbus in the cornea.[11,12] Interestingly, a significantly higher number of mast cells were seen to be distributed along the nasal limbus of the cornea. Furthermore, up-regulation of mast cell activation following suture placement was significantly higher on the nasal side compared with that on the temporal side, as indicated by increased levels of tryptase and β-hexosaminidase. On the basis of these observations, we postulated that the spatial distribution of mast cells contributes to the unequal nasal and temporal neovascularization.

To assess the effect of mast cell distribution on the asymmetrical angiogenic response, neovascularization was induced in mast cell−deficient cKit$^{w\text{-}sh}$ mice by placing a suture on the nasal or temporal side of the cornea. Of note, cKit$^{w\text{-}sh}$ mice, unlike other mast cell−deficient strain (cKit$^{w\text{-}v}$) that exhibits basal neutropenia and macrocytic anemia, do not have deficiency of other myeloid-derived cells, neutrophils, and macrophages, which are known to promote angiogenesis.[37−40] Interestingly, the noticeable dichotomy of nasal and temporal neovascularization in wild-type mice was not observed in mast cell−deficient mice, suggesting a critical role of mast cells in spatial angiogenic response at the ocular surface. Furthermore, the current data show considerably less neovascularization in cKit$^{w\text{-}sh}$ mice following suture placement, which is consistent with the previous finding of reduced vascular endothelial growth factor-A expression at the angiogenic site of mast cell−deficient mice.[16] Consistent with previous observations in cKit$^{w\text{-}sh}$ mice, the expression of angiogenic factors, including vascular endothelial growth factor-A and fibroblast growth factor (FGF2), was significantly down-regulated in cromolyn-treated mice, compared with PBS-treated controls (Supplemental Figure S2). Mast cell activation has been observed in various hypoxic tissue microenvironments, including hypoxic brain ischemia,[41] suggesting that mast cells may mediate the site-specific hypoxia-induced neovascularization, such as contact lens−induced superior pannus.[42,43]

In the translational arm of the study, whether pharmacologic inhibition of ocular surface mast cell activation abrogates the differences in the suture-induced nasal and temporal neovascularization was delineated. Following suture placement, corneas were topically treated with 2% cromolyn, a mast cell stabilizer that primarily prevents mast cell degranulation through direct membrane stabilization.[44] Topical administration of cromolyn effectively inhibits nonallergic ocular inflammation.[26,45] The current data show cromolyn treatment results in no significant difference in suture-induced neovascularization between the nasal and temporal side of the cornea, corroborating the observation in cKit$^{w\text{-}sh}$ mice. Additionally, cromolyn treatment resulted in significantly reduced corneal neovascularization. These findings suggest that mast cell blockade could be a potential therapeutic strategy to suppress neovascularization at the ocular surface and other vascularized organs, regardless of the site of the insult. Moreover, the current data showing a strong correlation between nasal mast cell distribution and neovascularization along with previous reports on increased mast cell density in promoting tumor angiogenesis suggest that tissue-specific immunologic niche may determine the severity of pathologic angiogenesis in different tissues.[46,47]

Taken together, our data demonstrate that the mast cells orchestrate site-specific neovascularization at the ocular surface and that inhibition of mast cell function abrogates the asymmetrical angiogenic response between the nasal and temporal portion of the cornea. These findings provide novel insights into the importance of the spatial distribution of mast cells in regulating the disproportionate pathologic growth of blood vessels.

Author Contributions

W.C., S.K.M., and S.K.C. assisted in designing the study, W.C. and E.E. performed experiments, W.C., S.K.M., and S.K.C. analyzed the data, and W.C., S.K.M., and S.K.C. wrote the manuscript. S.K.C. contributed the underlying hypothesis.

Supplemental Data

Supplemental material for this article can be found at *http://doi.org/10.1016/j.ajpath.2021.02.016*.

References

1. Foulsham W, Coco G, Amouzegar A, Chauhan SK, Dana R: When clarity is crucial: regulating ocular surface immunity. Trends Immunol 2018, 39:288−301
2. Cursiefen C, Chen L, Saint-Geniez M, Hamrah P, Jin Y, Rashid S, Pytowski B, Persaud K, Wu Y, Streilein JW, Dana R: Nonvascular VEGF receptor 3 expression by corneal epithelium maintains avascularity and vision. Proc Natl Acad Sci U S A 2006, 103: 11405−11410

3. Feizi S, Azari AA, Safapour S: Therapeutic approaches for corneal neovascularization. Eye Vis (Lond) 2017, 4:28
4. Chen Y, Chauhan SK, Lee HS, Stevenson W, Schaumburg CS, Sadrai Z, Saban DR, Kodati S, Stern ME, Dana R: Effect of desiccating environmental stress versus systemic muscarinic AChR blockade on dry eye immunopathogenesis. Invest Ophthalmol Vis Sci 2013, 54:2457−2464
5. Azar DT: Corneal angiogenic privilege: angiogenic and antiangiogenic factors in corneal avascularity, vasculogenesis, and wound healing (an American Ophthalmological Society thesis). Trans Am Ophthalmol Soc 2006, 104:264−302
6. Dolezalova V: Is the occurrence of a temporal pterygium really so rare? Ophthalmologica 1977, 174:88−91
7. Kaufman SC, Jacobs DS, Lee WB, Deng SX, Rosenblatt MI, Shtein RM: Options and adjuvants in surgery for pterygium: a report by the American Academy of Ophthalmology. Ophthalmology 2013, 120:201−208
8. Riedl JC, Wasielica-Poslednik J, Weyer-Elberich V, Vossmerbaeumer U, Pfeiffer N, Lisch W, Gericke A: Visualization of corneal vascularization in peripheral hypertrophic subepithelial corneal opacification with OCT angiography. Acta Ophthalmol 2018, 96: e974−e978
9. Norrby K: Mast cells and angiogenesis. APMIS 2002, 110:355−371
10. Krystel-Whittemore M, Dileepan KN, Wood JG: Mast cell: a multifunctional master cell. Front Immunol 2016, 6:620
11. Liu J, Fu T, Song F, Xue Y, Xia C, Liu P, Wang H, Zhong J, Li Q, Chen J, Li Y, Cai D, Li Z: Mast cells participate in corneal development in mice. Sci Rep 2015, 5:17569
12. Leonardi A, Motterle L, Bortolotti M: Allergy and the eye. Clin Exp Immunol 2008, 1(153 Suppl):17−21
13. Wernersson S, Pejler G: Mast cell secretory granules: armed for battle. Nat Rev Immunol 2014, 14:478−494
14. Ribatti D, Crivellato E: Mast cells, angiogenesis, and tumour growth. Biochim Biophys Acta 2012, 1822:2−8
15. Matsuda K, Okamoto N, Kondo M, Arkwright PD, Karasawa K, Ishizaka S, Yokota S, Matsuda A, Jung K, Oida K, Amagai Y, Jang H, Noda E, Kakinuma R, Yasui K, Kaku U, Mori Y, Onai N, Ohteki T, Tanaka A, Matsuda H: Mast cell hyperactivity underpins the development of oxygen-induced retinopathy. J Clin Invest 2017, 127:3987−4000
16. Cho W, Mittal SK, Elbasiony E, Chauhan SK: Activation of ocular surface mast cells promotes corneal neovascularization. Ocular Surface 2020, 18:857−864
17. Grimbaldeston MA, Chen CC, Piliponsky AM, Tsai M, Tam SY, Galli SJ: Mast cell-deficient W-sash c-kit mutant Kit W-sh/W-sh mice as a model for investigating mast cell biology in vivo. Am J Pathol 2005, 167:835−848
18. Elbasiony E, Mittal SK, Foulsham W, Cho W, Chauhan SK: Epithelium-derived IL-33 activates mast cells to initiate neutrophil recruitment following corneal injury. Ocular Surface 2020, 18: 633−640
19. Nigrovic PA, Gray DHD, Jones T, Hallgren J, Kuo FC, Chaletzky B, Gurish M, Mathis D, Benoist C, Lee DM: Genetic inversion in mast cell-deficient (Wsh) mice interrupts corin and manifests as hematopoietic and cardiac aberrancy. Am J Pathol 2008, 173:1693−1701
20. Jin Y, Chauhan SK, El Annan J, Annan JE, Sage PT, Sharpe AH, Dana R: A novel function for programmed death ligand-1 regulation of angiogenesis. Am J Pathol 2011, 178:1922−1929
21. Saban DR, Bock F, Chauhan SK, Masli S, Dana R: Thrombospondin-1 derived from APCs regulates their capacity for allosensitization. J Immunol 2010, 185:4691−4697
22. Summers SA, Gan PY, Dewage L, Ma FT, Ooi JD, O'Sullivan KM, Nikolic-Paterson DJ, Kitching AR, Holdsworth SR: Mast cell activation and degranulation promotes renal fibrosis in experimental unilateral ureteric obstruction. Kidney Int 2012, 82: 676−685
23. Wolf AJ, Reyes CN, Liang W, Becker C, Shimada K, Wheeler ML, Cho HC, Popescu NI, Coggeshall KM, Arditi M, Underhill DM: Hexokinase is an innate immune receptor for the detection of bacterial peptidoglycan. Cell 2016, 166:624−636
24. Chauhan SK, Jin Y, Goyal S, Lee HS, Fuchsluger TA, Lee HK, Dana R: A novel pro-lymphangiogenic function for Th17/IL-17. Blood 2011, 118:4630−4634
25. Ferrari G, Hajrasouliha AR, Sadrai Z, Ueno H, Chauhan SK, Dana R: Nerves and neovessels inhibit each other in the cornea. Invest Ophthalmol Vis Sci 2013, 54:813−820
26. Sahu SK, Mittal SK, Foulsham W, Li M, Sangwan VS, Chauhan SK: Mast cells initiate the recruitment of neutrophils following ocular surface injury. Invest Ophthalmol Vis Sci 2018, 59:1732−1740
27. Chung ES, Saban DR, Chauhan SK, Dana R: Regulation of blood vessel versus lymphatic vessel growth in the cornea. Invest Ophthalmol Vis Sci 2009, 50:1613−1618
28. Giacomini C, Ferrari G, Bignami F, Rama P: Alkali burn versus suture-induced corneal neovascularization in C57BL/6 mice: an overview of two common animal models of corneal neovascularization. Exp Eye Res 2014, 121:1−4
29. Coussens LM, Raymond WW, Bergers G, Laig-Webster M, Behrendtsen O, Werb Z, Caughey GH, Hanahan D: Inflammatory mast cells up-regulate angiogenesis during squamous epithelial carcinogenesis. Genes Dev 1999, 13:1382−1397
30. Moon TC, Befus AD, Kulka M: Mast cell mediators: their differential release and the secretory pathways involved. Front Immunol 2014, 5: 569
31. Altounyan RE: Review of clinical activity and mode of action of sodium cromoglycate. Clin Allergy 1980, (10 Suppl):481−489
32. Clements JL, Dana R: Inflammatory corneal neovascularization: etiopathogenesis. Semin Ophthalmol 2011, 26:235−245
33. Chauhan SK, Dohlman TH, Dana R: Corneal lymphatics: role in ocular inflammation as inducer and responder of adaptive immunity. J Clin Cell Immunol 2014, 5:1000256
34. Chan CML, Chew PTK, Alsagoff Z, Wong JS, Tan DTH: Vascular patterns in pterygium and conjunctival autografting: a pilot study using indocyanine green anterior segment angiography. Br J Ophthalmol 2001, 85:350−353
35. Woolley DE: The mast cell in inflammatory arthritis. N Engl J Med 2003, 348:1709−1711
36. Chen Y, Li C, Xie H, Fan Y, Yang Z, Ma J, He D, Li L: Infiltrating mast cells promote renal cell carcinoma angiogenesis by modulating PI3K→AKT→GSK3beta→AM signaling. Oncogene 2017, 36: 2879−2888
37. Zhou JS, Xing W, Friend DS, Austen KF, Katz HR: Mast cell deficiency in Kit(W-sh) mice does not impair antibody-mediated arthritis. J Exp Med 2007, 204:2797−2802
38. Tazzyman S, Lewis CE, Murdoch C: Neutrophils: key mediators of tumour angiogenesis. Int J Exp Pathol 2009, 90:222−231
39. Christoffersson G, Vågesjö E, Vandooren J, Lidén M, Massena S, Reinert RB, Brissova M, Powers AC, Opdenakker G, Phillipson M: VEGF-A recruits a proangiogenic MMP-9-delivering neutrophil subset that induces angiogenesis in transplanted hypoxic tissue. Blood 2012, 120:4653−4662
40. Carmi Y, Voronov E, Dotan S, Lahat N, Rahat MA, Fogel M, Huszar M, White MR, Dinarello CA, Apte RN: The role of macrophage-derived IL-1 in induction and maintenance of angiogenesis. J Immunol 2009, 183:4705−4714
41. Jin Y, Silverman AJ, Vannucci SJ: Mast cells are early responders after hypoxia-ischemia in immature rat brain. Stroke 2009, 40: 3107−3112
42. Efron N: Contact Lens Practice. Edited by Effron N. 3rd ed. Melbourne, Australia: Elsevier, 2018. pp. 496
43. Chang JH, Gabison EE, Kato T, Azar DT: Corneal neovascularization. Curr Opin Ophthalmol 2001, 12:242−249
44. Kneilling M, Hültner L, Pichler BJ, Mailhammer R, Morawietz L, Solomon S, Eichner M, Sabatino J, Biedermann T, Krenn V,

Weber WA, Illges H, Haubner R, Röcken M: Targeted mast cell silencing protects against joint destruction and angiogenesis in experimental arthritis in mice. Arthritis Rheum 2007, 56:1806−1816

45. Li M, Mittal SK, Foulsham W, Amouzegar A, Sahu SK, Chauhan SK: Mast cells contribute to the induction of ocular mucosal alloimmunity. Am J Transplant 2019, 19:662−673

46. Takanami I, Takeuchi K, Naruke M: Mast cell density is associated with angiogenesis and poor prognosis in pulmonary adenocarcinoma. Cancer 2000, 88:2686−2692

47. Dundar E, Oner U, Peker BC, Metintas M, Isiksoy S, Ak G: The significance and relationship between mast cells and tumour angiogenesis in non-small cell lung carcinoma. J Int Med Res 2008, 36:88−95